(80 mL) were added in alternate portions of 5–10 mL. The product was worked up as described above for 4 and 5 to yield 0.62 g (29%) of 8 after crystallization from acetone: mp 92–93 °C; $^1$H NMR (8:1 methylcyclohexane-$d_{14}$/toluene-$d_8$) δ 1.06 (t, 18 H, $^3J$ = 7.3 Hz), 2.74 (s, 18 H), 3.11 (q, 12 H, $^3J$ = 7.3 Hz); $^{13}$C NMR ($CD_2Cl_2$) δ 10.11 ($CH_2CH_3$), 44.96 ($NCH_3$), 48.40 ($CH_2CH_3$), 150.55, 151.37 ($C_{ar}$). Anal. Calcd for $C_{24}H_{48}N_6$: C, 68.52; H, 11.50; N, 19.98. Found: C, 68.03; H, 11.82; N, 19.94.

**Hexakis(diethylamino)benzene (10).** 1,3,5-Tris(diethylamino)-2,4,6-trinitrobenzene was reduced as described above and then ethylated in water with a 10-fold excess of ethyl trifluoromethanesulfonate added in alternate portions, with enough 10 M sodium hydroxide solution to keep the mixture strongly basic. The mixture was stirred for 30 min and extracted with ether. The ether extracts were combined and dried over magnesium sulfate, and the ether was evaporated to give a brown residue. Crystallization from acetone gave the desired product: mp 211–213 °C; $^1$H NMR (methylcyclohexane-$d_{14}$) δ 0.97 (t, 18 H, $^3J$ = 7.3 Hz), 3.12 (q, 12 H, $^3J$ = 7.3 Hz); $^{13}$C NMR (methylcyclohexane-$d_{14}$) δ 15.58 ($CH_2CH_3$), 50.72 ($CH_2CH_3$), 152.70 ($C_{ar}$); mass spectrum (high resolution), $m/z$ 504.4889 (504.4879 calcd for $C_{30}H_{60}N_6$).

**1,3,5-Tris(ethylmethylamino)-2,4,6-tris(dimethylamino)benzene (11).** 1,3,5-Tris(ethylamino)-2,4,6-trinitrobenzene was prepared by the method of Mustafa and Zahran,[28] mp 206–207 °C (lit.[28] mp 206 °C). The compound was reduced by the method of Rogers[8] and methylated as described for hexakis(dimethylamino)benzene. An identical workup, followed by crystallization from acetone, gave white, chunky crystals: mp 121.5–122.5 °C; $^1$H NMR (methylcyclohexane-$d_{14}$) δ 1.14 (t, 9 H, $^3J$ = 7.2 Hz), 2.66 (s, 9 H), 2.99 (s, 18 H), 3.05 (q, 6 H, $^3J$ = 7.2 Hz); $^{13}$C NMR (toluene-$d_8$/methylcyclohexane-$d_{14}$, 3:1) δ 14.30 ($CH_2CH_3$), 41.52 ($EtNCH_3$), 45.16 ($N(CH_3)_2$), 51.14 ($CH_2CH_3$), 151.93, 154.06 ($C_{ar}$); mass spectrum (high resolution), $m/z$ 378.3464 (378.3471 calcd for $C_{21}H_{42}N_6$).

**X-ray Crystallography.** Crystals of 4 were obtained by slow evaporation from acetone. A crystal of approximately 0.26 × 0.26 × 0.52 mm$^3$ was chosen for the X-ray measurements. Crystal data: $C_{18}H_{36}N_6$, $M$ = 336.6 g·mol$^{-1}$; monoclinic (space group $C2/c$); $a$ = 18.440 (6) Å, $b$ = 9.461 (3) Å, $c$ = 12.017 (4) Å, and $\beta$ = 104.74 (3)°, $V$ = 2027 (1) Å$^3$, $d_{calcd}$ = 1.10 g·cm$^{-3}$, $Z$ = 4. X-ray intensities were collected at 175 ± 3 K on a Nicolet R3m four-circle diffractometer equipped with a nitrogen-flow cooling device by applying Mo Kα radiation (λ = 0.71069 Å). A total of 1794 independent reflections were recorded with $3° \le 2\theta \le 50°$ of which 1500 with $[|F_o| > 3\sigma(F_o)]$ were considered unique and observed. The structure was solved by direct methods with the SHELXTL software. Carbon and nitrogen atoms were refined with anisotropic thermal parameters. All hydrogen atoms were included in the refinement at idealized positions (C–H = 0.96 Å, N–C–H = 109.5°) and were refined isotropically by using a riding model. $R$ and $R_w$ factors after refinement were 0.048 and 0.055, respectively.

Crystals of 5 and 8 suitable for X-ray analysis were grown from acetone and 1:1 methanol/dichloromethane, respectively. The thin needles of 8 were extremely brittle and diffracted very poorly at $2\theta > 40°$. Crystal data and structural parameters for 5 and 8 are given in ref 18 and in the supplementary material, respectively.

**Acknowledgment.** We thank the National Science Foundation (CHE-8510067) for support of this work.

**Registry No.** 4, 114396-17-7; 4·TCNQ, 114422-55-8; 5, 114422-56-9; 7, 114396-19-9; 8, 114396-21-3; 9, 114396-22-4; 10, 114396-23-5; 11, 114396-24-6; hexaaminobenzene, 4444-26-2; 1,3,5-trinitro-2,4,6-triaminobenzene, 3058-38-6; 1,3,5-trichloro-2,4,6-trinitrobenzene, 2631-68-7; 1,3,5-tris(diethylamino)-2,4,6-trinitrobenzene, 114396-18-8; 1,3,5-tris(ethylamino)-2,4,6-trinitrobenzene, 91881-07-1.

**Supplementary Material Available:** Bond lengths and bond angles with standard deviations, anisotropic thermal parameters, hydrogen atom coordinates for 4 (Tables IV–VII); crystal parameters, data measurements, atomic coordinates, bond lengths and bond angles with standard deviations, anisotropic thermal parameters for 8 (Tables VIII–XIV) (8 pages). Structure factor tables are available from the author. Ordering information is given on any current masthead page.

---

# Ab Initio Calculations of Hydrogen Transfers. A Computational Test of Variations in the Transition-State Structure and the Coefficient of Rate-Equilibrium Correlation

Hiroshi Yamataka*,[1a] and Shigeru Nagase*,[1b]

*The Institute of Scientific and Industrial Research, Osaka University, Ibaraki, Osaka 567, Japan, and Department of Chemistry, Faculty of Education, Yokohama National University, Hodogaya, Yokohama 240, Japan*

*Received October 8, 1987*

Hydrogen atom transfers from R–H (R = Me, Et, *i*-Pr, or *t*-Bu) to X$^\bullet$ (X = H or Cl) were investigated by using the ab initio molecular orbital method with the object of gaining insight into the relation between transition-state (TS) structures and reactivities and into the significance of the coefficient, α, of rate–equilibrium correlation. Structures of the reactants, TSs, products, and σ complexes were fully optimized with the 3-21G basis set. Single-point energy calculations were carried out for all the structures at the MP2/6-31G* level. It was found that the TS structure becomes more reactant-like for a more reactive R–H when X = H while it is unchanged when X = Cl. The $\Delta E^\ddagger$–$\Delta E$ correlation gave straight lines with slopes of 1.0 and 1.4 respectively for X = H and Cl. These results were discussed in terms of Marcus' equation. It was concluded that (1) the coefficient α is an experimentally (or computationally) derived index of selectivity but not always a reliable measure of the TS structure, (2) the variation in the intrinsic barrier is an important factor in determining the magnitude of α, and (3) the α value becomes anomalously sizable when a new interaction occurs between the two reacting fragments in the TS and therefore the arithmetic mean assumption breaks down.

Correlation between rates and equilibria (eq 1) is one of the most commonly used free energy relationships in organic chemistry, and the coefficient α has usually been taken as a measure of the position of the transition state (TS) along the reaction coordinate. When the TS has an

$$\log k = \alpha \log K + C \qquad (1)$$

intermediate character between the reactant and the product, the value of α should be between 0.0 and 1.0. The Hammond postulate[2] and its Leffler[3] generalization pro-

---

[1] (a) Osaka University. (b) Yokohama National University.

**Table I. Selected TS Bond Lengths and Activation and Reaction Energies for the Hydrogen-Transfer Reactions**

| | Me- -H- -H[g] | Et- -H- -H | Pr- -H- -H | Bu- -H- -H | Me- -H- -Cl[h] | Et- -H- -Cl | Pr- -H- -Cl | Bu- -H- -Cl |
|---|---|---|---|---|---|---|---|---|
| $r_{C\text{-}H}$[a] | 1.371 | 1.355 | 1.341 | 1.330 | 1.498 | 1.489 | 1.486 | 1.496 |
| $r_{H\text{-}X}$[a] | 0.926 | 0.938 | 0.947 | 0.953 | 1.453 | 1.458 | 1.457 | 1.450 |
| $n_{C\text{-}H}$[b] | 0.380 | 0.405 | 0.426 | 0.443 | 0.251 | 0.259 | 0.263 | 0.255 |
| $n_{H\text{-}X}$[b] | 0.529 | 0.508 | 0.493 | 0.484 | 0.589 | 0.579 | 0.581 | 0.595 |
| $\Delta E^{\ddagger}$[c] | 25.6 | 22.8 | 20.36 | 18.1 | 18.4 | 13.0 | 8.3 | 4.2 |
| $\Delta E$[d] | 11.2 | 8.3 | 5.7 | 3.8 | 15.0 | 12.1 | 9.5 | 7.6 |
| $\Delta E$[e] | | | | | 12.6 | 8.6 | 5.1 | 2.2 |
| $X^{*}$[f] | 0.64 | 0.61 | 0.58 | 0.56 | 0.76 | 0.75 | 0.72 | 0.68 |

[a] HF/3-21G-optimized distance in angstroms. [b] Pauling's bond order calculated by eq 9. [c] Activation energy at MP2/6-31G*//3-21G. [d] Reaction energy at MP2/6-31G*//3-21G in kcal/mol defined by the energy difference between the products and the reactants. [e] Reaction energy at MP2/6-31G*//3-21G in kcal/mol defined by the energy difference between the complex and the reactants. [f] Miller's TS index calculated by eq 10. [g] $\Delta E^{\ddagger}$ and $\Delta E$ at MP3/6-31G**//6-31G** are 22.6 and 4.9 kcal/mol; the experimental energies[18] are 11.8 and −1.0 kcal/mol, respectively. [h] $\Delta E^{\ddagger}$ and $\Delta E$ at MP3/6-31G**//6-31G** are 16.1 and 9.0 kcal/mol; experimental values[19] are 3.9 and −1.1 kcal/mol, respectively.

vided the theoretical basis for $\alpha$ as a transition index. A more quantitative means of interpreting the $\alpha$ value was given by Marcus' equation (eq 2), in which $\Delta E^{\ddagger}$ and $\Delta E$ have their usual meanings and $\Delta E_0^{\ddagger}$ is the intrinsic barrier, the barrier of the hypothetical thermoneutral reaction.[4] From the equation, $\alpha$ can be obtained by eq 3 on condition that $\Delta E_0^{\ddagger}$ is independent of $\Delta E$. A large number of experimental data have successfully been treated with eq 2 and 3.

$$\Delta E^{\ddagger} = \Delta E_0^{\ddagger} + \frac{1}{2}\Delta E + \frac{(\Delta E)^2}{16\Delta E_0^{\ddagger}} \tag{2}$$

$$\alpha = \frac{\partial \Delta E^{\ddagger}}{\partial \Delta E} = \frac{1}{2} + \frac{\Delta E}{8\Delta E_0^{\ddagger}} \tag{3}$$

Recently, Kreevoy[5] and Lewis[6] developed a modified treatment of Marcus' equation in which the magnitude of the intrinsic barrier was allowed to vary for a series of reactions. Under the situation that $\Delta E_0^{\ddagger}$ is a function of $\Delta E$,[4,7] eq 2 gives eq 4. If $1 \gg (1/16)(\Delta E/\Delta E_0^{\ddagger})^2$, then eq 4 gives eq 5. The first two terms of eq 5 are the same as

$$\frac{\partial \Delta E^{\ddagger}}{\partial \Delta E} = \frac{1}{2} + \frac{\Delta E}{8\Delta E_0^{\ddagger}} + \left[1 - \frac{1}{16}\left(\frac{\Delta E}{\Delta E_0^{\ddagger}}\right)^2\right]\frac{\partial \Delta E_0^{\ddagger}}{\partial \Delta E} \tag{4}$$

$$\frac{\partial \Delta E^{\ddagger}}{\partial \Delta E} = \frac{1}{2} + \frac{\Delta E}{8\Delta E_0^{\ddagger}} + \frac{\partial \Delta E_0^{\ddagger}}{\partial \Delta E} \tag{5}$$

in eq 3, and the third term is an additional term arising from the situation that $\Delta E_0^{\ddagger}$ is dependent on $\Delta E$. The third term provides reasoning for often-cited observations[8-10] that the $\alpha$ value is not 0.5 at $\Delta E = 0$ as predicted by eq 3. Equation 5 suggests that the apparent $\alpha$ value ($\alpha_A$) is the sum of the conventional term from eq 3 ($\alpha_C$) and the term arising from the variation of the intrinsic barrier ($\alpha_I$). This version was successfully applied to experimental results, and the value $\partial \Delta E_0^{\ddagger}/\partial \Delta E$ (originally in a free energy term) was taken as a measure of the tight–loose character of the TS.[5,6]

In the present paper, we report results of a computational test in a model reaction system with the aim of clarifying the origin of the $\alpha$ variation. The Kreevoy–Lewis treatment was applied to the present results as well as the available results in the literature from both experimental and computational sources.[11] We also discuss the relation between $\alpha$ and the TS structure, which are often assumed to vary in a similar manner.

## Computational Method and Results

Ab initio MO calculations were carried out[12,13] for hydrogen atom transfers from R–H to X$^{\bullet}$ (eq 6)[14] and the symmetry reactions (eq 7 and 8). Hypothetical bound

$$\text{R–H} + \text{X}^{\bullet} \rightarrow \text{R}^{\bullet} + \text{H–X} \tag{6}$$

$$\text{R–H} + \text{R}^{\bullet} \rightarrow \text{R}^{\bullet} + \text{H–R} \tag{7}$$

$$\text{X–H} + \text{X}^{\bullet} \rightarrow \text{X}^{\bullet} + \text{H–X} \tag{8}$$

$$\text{R} = CH_3,\ CH_3CH_2,\ (CH_3)_2CH,\ (CH_3)_3C$$

$$\text{X} = \text{H}^{\bullet},\ \text{Cl}^{\bullet}$$

species, [R–H–X]$^{\bullet}$, which correspond to reference compounds in the More O'Ferrall potential energy diagram treatment,[15] were also calculated; here the geometries of R–H and H–X were taken to be the same as those in the separated species, and only the R–H–X angle was optimized. All species in the stationary points were optimized at the spin-unrestricted Hartree–Fock (HF) level with the 3-21G basis set[16a] by using the energy gradients. The TSs were confirmed in the R = $CH_3$ cases by vibrational frequency calculations, which gave only one imaginary frequency in each case. Energies were calculated on the

---

(2) Hammond, G. S. *J. Am. Chem. Soc.* **1955**, *77*, 334.

(3) Leffler, J. E. *Science* (*Washington, D.C.*) **1953**, *117*, 340.

(4) Marcus, R. A. *J. Phys. Chem.* **1968**, *72*, 891. Cohen, A. O.; Marcus, R. A. *Ibid.* **1968**, *72*, 4244. Marcus, R. A. *J. Am. Chem. Soc.* **1969**, *91*, 7224.

(5) Kreevoy, M. M.; Lee, I.-S. H. *J. Am. Chem. Soc.* **1984**, *106*, 2550.

(6) Lewis, E. S.; Hu, D. D. *J. Am. Chem. Soc.* **1984**, *106*, 3292. Lewis, E. S. *J. Phys. Chem.* **1986**, *90*, 3756.

(7) Murdoch, J. R.; Magnoli, D. E. *J. Am. Chem. Soc.* **1982**, *104*, 3792.

(8) Wiseman, F.; Kestner, N. R. *J. Phys. Chem.* **1984**, *88*, 4354.

(9) Kondo, Y.; Zanka, A.; Kusabayashi, S. *J. Chem. Soc., Perkin Trans. 2* **1985**, 827.

(10) (a) Lewis, E. S.; Kukes, S. *J. Am. Chem. Soc.* **1979**, *101*, 417. (b) Lewis, E. S.; Yousaf, T. I.; Douglas, T. A. *Ibid.* **1987**, *109*, 2152.

(11) Although the experimental results are on the free energy basis while those of MO calculations in model reactions are in terms of potential energy, the difference will, we believe, cause no serious trouble in the final conclusions.

(12) GAUSSIAN 80 program: Binkley, J. S.; Whiteside, R. A.; Krishnan, R.; Seeger, R.; DeFrees, D. J.; Schlegel, H. B.; Topiol, S.; Kaln, L. R.; Pople, J. A. QCPE 406; Indiana University: Bloomington, IN, 1980.

(13) GAUSSIAN 82 program: Binkley, J. S.; Frisch, M. J.; DeFrees, D. J.; Raghavachari, K.; Whiteside, R. A.; Schlegel, H. B.; Flunder, E. M.; Pople, J. A. Carnegie-Mellon University: Pittsburgh, PA.

(14) Some MO calculations have been reported for the reactions: Ehrenson, S.; Newton, M. D. *Chem. Phys. Lett.* **1972**, *13*, 24. Motell, E. L.; Fink, W. H. *J. Am. Chem. Soc.* **1976**, *98*, 7152. Rayez-Meaume, M. T.; Dannenberg, J. J.; Whitten, J. L. *J. Am. Chem. Soc.* **1978**, *100*, 747. Wildman, T. A. *Chem. Phys. Lett.* **1986**, *126*, 325. Lee, B.-S.; Lee, I.; Song, C. H.; Choi, J. Y. *J. Comput. Chem.* **1985**, *6*, 486.

(15) More O'Ferrall, R. A. *J. Chem. Soc. B* **1970**, 274.

(16) (a) 3-21G: Binkley, J. S.; Pople, J. A.; Hehre, W. J. *J. Am. Chem. Soc.* **1980**, *102*, 939. Gordon, M. S.; Binkley, J. S.; Pople, J. A.; Pietro, W. J.; Hehre, W. J. *J. Am. Chem. Soc.* **1982**, *104*, 2797. (b) 6-31G* and 6-31G**: Hehre, W. J.; Ditchfield, R.; Pople, J. A. *J. Chem. Phys.* **1972**, *56*, 2257. Hariharan, P. C.; Pople, J. A. *Theor. Chim. Acta* **1973**, *28*, 213. Francl, M. M.; Pietro, W. J.; Hehre, W. J.; Binkley, J. S.; Gordon, M. S.; DeFrees, D. J.; Pople, J. A. *J. Chem. Phys.* **1982**, *77*, 3654.

**Table II. Selected Bond Lengths and Activation Energies for the Symmetry Reactions**

| | Me- -H- -Me | Et- -H- -Et | Pr- -H- -Pr | Bu- -H- -Bu | H- -H- -H |
|---|---|---|---|---|---|
| $r_{C-H}{}^{a}$ | 1.356 | 1.355 | 1.354 | 1.355 | 0.943[e] |
| $n_{C-H}{}^{b}$ | 0.403 | 0.405 | 0.408 | 0.408 | 0.515 |
| $\Delta E^{\ddagger c}$ | 22.4[d] | 20.5 | 18.2 | 15.3 | 17.2 |

[a-c] See footnotes *a–c* in Table I. [d] $\Delta E$ at MP3/6-31G**//6-31G** is 25.2 kcal/mol; experimental value[20] is 14.7 kcal/mol. [e] $r_{H-H}$, in angstroms.

**Scheme I**

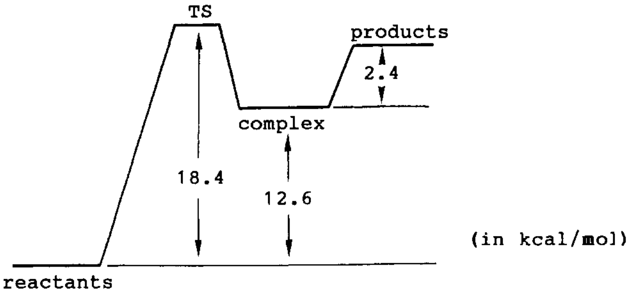

HF/3-21G-optimized geometries with the second-order Møller–Ploesset perturbation theory (MP2)[17] and the larger 6-31G* basis set,[16b] these denoted by MP2/6-31G*//3-21G. For three of the reactions, i.e., $CH_3–H + H^{\bullet}$, $CH_3–H + CH_3{}^{\bullet}$, and $CH_3–H + Cl^{\bullet}$, a higher level of calculations was also carried out at MP3/6-31G**//6-31G**.[16b,17] The calculated TS geometry was nearly the same regardless of the basis set (3-21G vs 6-31G**) for the first two reactions, but was substantially different for the reaction with $Cl^{\bullet}$; the C- -H bond is 0.14 Å shorter and the C- -Cl bond is 0.04 Å longer with the 6-31G** basis set. The barrier height was essentially independent of the level of calculations (MP2/6-31G*//3-21G vs MP3/6-31G**//6-31G**) while the reaction energy was subject to the method; the reactions are calculated to be less endothermic at the MP3/6-31G**//6-31G** level. The results are shown in Table I. Although the present level of calculations does not seem to be credible enough for practical evaluation of activation and reaction energies, we believe that qualitative comparison is valid for a homologous series of reactions and that the analysis of the model reactions may well be applied to a real system.

Tables I and II list selected structural features of the TSs as well as the activation and reaction energies. Table III summarizes the energy of the hypothetical species necessary for the More O'Ferrall treatment relative to the reactant state.

It is interesting to note that the hydrogen transfer from R to X involves the formation of a σ complex before reaching the product state when X = Cl. Such a hydrogen-bonded complex has experimentally been detected when X = F.[21] The energy profile for the reaction of Me–H with $Cl^{\bullet}$ is shown in Scheme I. The C–H and H–Cl bond lengths of the complex are 2.283 and 1.302 Å, which correspond to Pauling bond orders (eq 9), $n_P$, of 0.02 and 0.97, respectively.[22] The σ complexes are 2–5 kcal/mol

$$\ln n_P = \frac{1}{0.3}(R_0 - R) \qquad (9)$$

more stable than the separated products, and therefore the process from the reactants to the complexes will be considered for X = Cl in the following discussion. The complex formation was not observed for the reactions with $H^{\bullet}$.

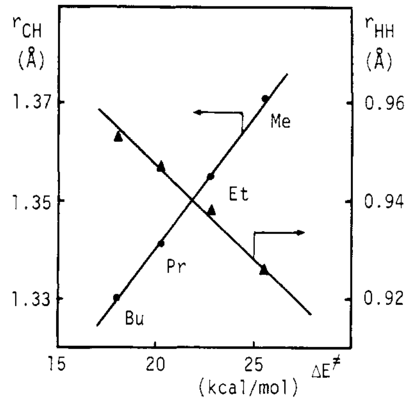

**Figure 1.** Plots of the C–H and H–H bond lengths in the TS, [R- -H- -H], vs the calculated barrier height.

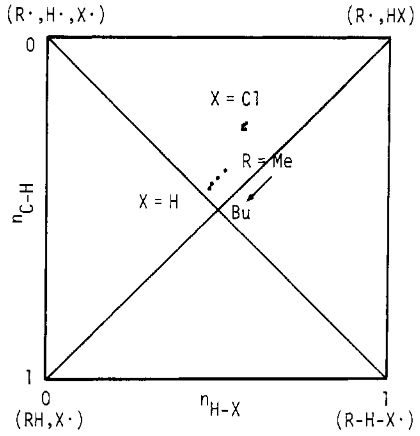

**Figure 2.** More O'Ferrall diagram for the hydrogen-transfer reactions.

## Discussion

**Structure of the Transition State.** The structure of the TS in the reactions of R–H with $H^{\bullet}$ varies in a regular manner with the change in R as shown in Table I and Figure 1. The more reactive R–H, the earlier the TS, as characterized by less lengthening of the C- -H bond and weaker formation of the H- -H bond; thus the Leffler–Hammond principle holds.[2,3] This is one of many examples in which a quantum mechanically calculated TS varies its structure with the change in reactivity in a manner expected for the Leffler–Hammond principle.[7,23-25] In Figure 2 is shown a More O'Ferrall-type diagram in terms of the Pauling bond orders of the reacting bonds.[15] Two points are noteworthy in Figure 2. First, in the case of X = H the TS lies near the diagonal line between the reactants and the products and shifts in a parallel fashion to it. As Tables I and III show, the change in the reaction energy (−7.4 kcal/mol = 3.8 − 11.2) when R is varied from Me to Bu is larger than the change in the relative energy of the two hypothetical states ($E_{[R-H-H]^{\bullet}} - E_{[R^{\bullet},H^{\bullet},H^{\bullet}]}$) for the same variation in R (−3.1 kcal/mol = (50.5 − 104.3) − (45.8 −

---

[17] MP2: Binkley, J. S.; Pople, J. A. *Int. J. Quantum Chem., Symp.* **1975**, *9*, 229. MP3: Pople, J. A.; Binkley, J. S.; Seeger, R. *Int. J. Quantum Chem., Symp.* **1976**, *10*, 1.

[18] Kurylo, M. J.; Timmons, R. B. *J. Chem. Phys.* **1969**, *50*, 5076.

[19] Eckling, G. C. R.; Goldfinger, P.; Huybrechts, G.; Johnston, H. S.; Meyers, L.; Verbeke, G. *J. Chem. Phys.* **1963**, *38*, 1053.

[20] Dainton, F. S.; Ivin, K. J.; Wilkinson, F. *Trans. Faraday Soc.* **1959**, *55*, 929.

[21] Jacox, M. E. *Chem. Phys.* **1979**, *42*, 133.

[22] Pauling, L. *J. Am. Chem. Soc.* **1947**, *69*, 542.

[23] Wolfe, S.; Mitchell, D. J.; Schlegel, H. B. *J. Am. Chem. Soc.* **1981**, *103*, 7692.

[24] Rondam, N. G.; Houk, K. N.; Moss, R. A. *J. Am. Chem. Soc.* **1980**, *102*, 1770.

[25] Scheiner, S.; Redfern, P. *J. Phys. Chem.* **1986**, *90*, 2969.

**Table III. Energy of the Hypothetical Species in the More O'Ferrall Diagram**[a]

| | | | | | | | |
|---|---|---|---|---|---|---|---|
| Me-H-H | Et-H-H | Pr-H-H | Bu-H-H | Me-H-Cl | Et-H-Cl | Pr-H-Cl | Bu-H-Cl |
| 50.5 | 48.9 | 47.3 | 45.8 | 44.9 | 40.9 | 37.4 | 34.4 |
| H-H-H | CH-H-Cl | Me-H-Me | H,H,X | Me,H,X | Et,H,X | Pr,H,X | Bu,H,X |
| 37.4 | 41.6 | 59.3 | 92.7 | 104.3 | 101.1 | 98.5 | 96.5 |

[a] MP3/6-31G*//3-21G energy relative to the reactant state, in kcal/mol.

**Table IV. Calculated Intrinsic Barrier for Reaction 6**[a]

| R | X = H | X = Cl |
|---|---|---|
| Me | 19.6 (19.8) | 11.2 |
| Et | 18.4 (18.9) | 8.1 |
| *i*-Pr | 17.3 (17.7) | 5.5 |
| *t*-Bu | 16.1 (16.3) | 3.0 |

[a] Calculated by eq 11 at MP2/6-31G*//3-21G, in kcal/mol. Figures in parentheses are those calculated by eq 12.

96.5)). Thus, the energy perturbation introduced by R is larger in the parallel direction than in the perpendicular one. It is well recognized that the geometrical response to the perturbation in energy is larger in the parallel direction than in the perpendicular one,[26] and therefore the observed shift of the TS position is consistent with the More O'Ferrall-type treatment. Second, in contrast to the cases of X = H, the TS structure is essentially unchanged with R when X = Cl. This shows that endothermicity is not the sole factor in controlling the extent of the TS variation, since the changes in endothermicity with R are similar for both series of reactions.

Equation 3, derived from Marcus' theory, predicts that the magnitude of the coefficient $\alpha$ varies to a smaller extent in reactions with larger intrinsic barriers for a given change in endothermicity. Thus, one might expect that the TS structure also varies to a smaller extent in reactions with a larger intrinsic barrier. However, the interpretation by use of eq 3 is not applicable to the present case since, as will be discussed later (see also Table IV), the intrinsic barrier is much smaller for X = Cl than H. Thornton has pointed out that a TS structure would shift to a lesser extent when the potential energy (PE) curvature along the perturbed vibrational mode is steeper.[26] Therefore it can be anticipated that the PE surface in the neighborhood of the TS is steeper for X = Cl. However, as indicated by the magnitude of the reaction-coordinate frequency ($\nu_L{}^{\ddagger} = 1300i$ cm$^{-1}$ for Cl and $2200i$ cm$^{-1}$ for H), the PE surface appears rather flat for X = Cl compared with that for X = H, and hence the steepness of the PE surface is not the origin of the invariance of the TS for X = Cl.

One possible cause of the different behavior of the TSs may lie in the different degree of charge separation at the TSs of these reactions. Population analysis showed that when X = H the reaction is essentially a radical process and the change in charge density on R is small and increases monotonically in going from R–H to the product, R$^{\bullet}$, through the TS, while in the reaction of R–H with Cl, considerable positive charge develops on R at the TS; R has a larger positive charge in the TS than in the product (vide infra). This means that energy perturbation introduced by the change in R increases monotonically along the reaction coordinate for X = H; thus the change in R from Me to Bu causes both a decrease of $\Delta E^{\ddagger}$ and a shift of the TS to a more reactant-like position at the same time. On the other hand, when X = Cl the energy perturbation may be concave upward along the reaction coordinate, and the size of perturbation can be nearly constant in the neighborhood of the TS. In such a case the change in R from Me to Bu results in the reduction of $\Delta E^{\ddagger}$ but may have little effect on the position of the TS. This is shown schematically in Figure 3.

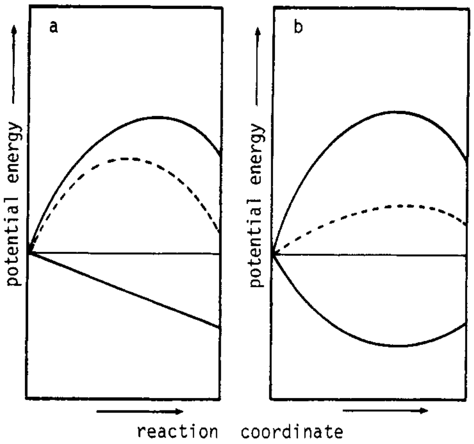

**Figure 3.** Schematic presentation of the perturbed PE reaction profiles (broken lines). The upper and the lower solid lines are the unperturbed PE reaction profiles and perturbations, respectively. (a) Linear perturbation; (b) concave perturbation.

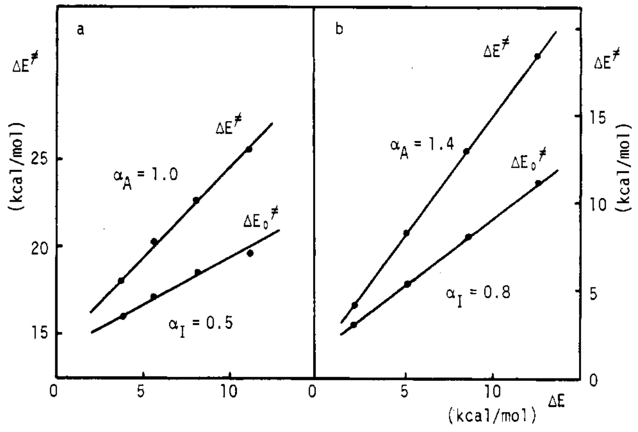

**Figure 4.** Plots of $\Delta E^{\ddagger}$ and $\Delta E_0{}^{\ddagger}$ vs $\Delta E$ for the reactions of R–H with X$^{\bullet}$: (a) X = H; (b) X = Cl.

It should be noted that, as eq 1 and 3 show, the $\alpha$ value is defined in terms of energy and therefore it is not necessarily related to the variation of the TS structure.[8,27] There are two relations: one between the TS structure and endothermicity, and the other between $\alpha$ and endothermicity. These relations are different by nature although they are often assumed to be parallel. Interestingly, Miller's index, $X^*$, defined by eq 10,[28] varies regularly with

$$X^* = \Delta E^{\ddagger}/(2\Delta E^{\ddagger} - \Delta E) \qquad (10)$$

the variation in R in both X = H and Cl cases (Table I). This shows that Miller's index also does not serve as a measure of the TS structure.

**Variation in the Coefficient $\alpha$.** The $\Delta E^{\ddagger}$–$\Delta E$ correlation is shown in Figure 4 for X = H and Cl. In both cases, excellent linear plots were obtained with slopes of 1.00 and 1.40, respectively (shown as $\alpha_A$). However, the

---

[26] Thornton, E. R. *J. Am. Chem. Soc.* **1967**, *89*, 2915.

[27] Firmoshinho, S. *J. Chem. Soc., Perkin Trans. 2* **1987**, 61.

[28] Miller, A. R. *J. Am. Chem. Soc.* **1978**, *100*, 1984.

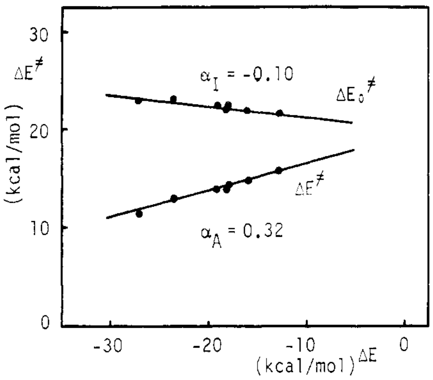

**Figure 5.** Plots of $\Delta E^{\ddagger}$ and $\Delta E_0^{\ddagger}$ vs $\Delta E$ for the reactions of $CH_3I$ with aromatic amines in acetonitrile.[9,31]

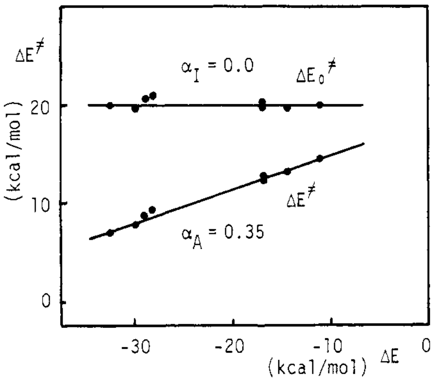

**Figure 6.** Plots of $\Delta E^{\ddagger}$ and $\Delta E_0^{\ddagger}$ vs $\Delta E$ for the reactions of $CH_3I$ with aliphatic amines in aceonitrile.[9]

size of the slopes is outside of the normal range (0–1), especially in the latter case. Clearly, $\alpha$ is not a reliable measure of the TS position along the reaction coordinate. Figure 4 also shows the plots of $\Delta E_0^{\ddagger}$ against $\Delta E$ for reaction 6. The $\Delta E_0^{\ddagger}$ values were obtained in two ways, first by eq 11, which can directly be obtained from Marcus' equation (eq 2),[29] and second by the assumption of arithmetic mean of two symmetry reactions, eq 12.[4] In the case

$$\Delta E_0^{\ddagger} = \tfrac{1}{2}\Delta E^{\ddagger} - \tfrac{1}{2}\Delta E + [\Delta E^{\ddagger}(\Delta E^{\ddagger} - \Delta E)]^{1/2} \quad (11)$$

$$\Delta E_0^{\ddagger}{}_{R,X} = \tfrac{1}{2}[(\Delta E^{\ddagger}{}_{R,R} + \Delta E^{\ddagger}{}_{X,X})] \quad (12)$$

of X = H, the two equations give similar intrinsic barriers, indicating that the assumption included in eq 12 is satisfied (Table IV); in other words, Marcus' equation reproduces the quantum mechanical activation barrier quite well. In the case of X = Cl, there is no symmetry reaction because of the complex formation and therefore only the values calculated by eq 11 are given in Table IV.

It is apparent that for X = H half of $\alpha_A$ comes from $\alpha_I$ and that $\alpha_C$ has a quite normal value of about 0.5. The same treatment can successfully be applied to many other reaction systems both from experimental and theoretical sources.[9,24,27,30-33] Some of the results are shown in Figures 5–9. In all but one case, $\alpha_I$ is not zero, indicating that the experimentally derived $\alpha$ value is a composite quantity.

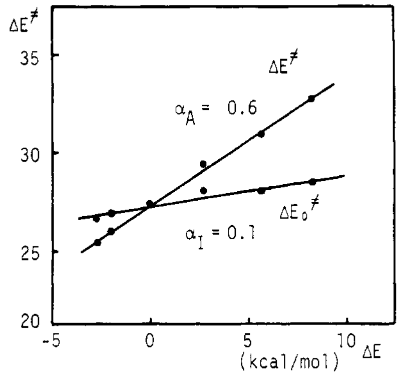

**Figure 7.** Plots of $\Delta E^{\ddagger}$ and $\Delta E_0^{\ddagger}$ vs $\Delta E$ for the reactions of $CH_3SPh$ with $ArS^-$ in ethanol.[10a]

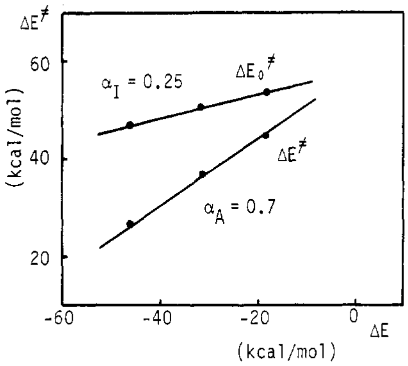

**Figure 8.** Plots of $\Delta E^{\ddagger}$ and $\Delta E_0^{\ddagger}$ vs $\Delta E$ for the addition reactions of :CXY to $C_2H_4$ calculated by the ab initio SCF method with the 4-31G basis set.[24]

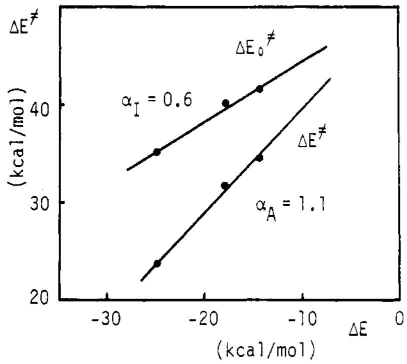

**Figure 9.** Plots of $\Delta E^{\ddagger}$ and $\Delta E_0^{\ddagger}$ vs $\Delta E$ for the addition reactions of $NR_2H$ to $H_2C{=}O$ calculated by the ab initio SCF method with the 3-21G basis set.[32]

Furthermore, it is interesting to see that $\alpha_C$ is in most cases close to 0.5, in contrast to the larger variation in $\alpha_A$.

The factor controlling the magnitude of $\alpha_I$ has been presented previously,[5,6] but let us discuss it briefly. Under the arithmetic mean assumption, the intrinsic barrier of reaction 6, R–H + X → R + H–X, is given by eq 12. The variation in the $\Delta E_0^{\ddagger}{}_{R,X}$ with R is then given by

$$d(\Delta E_0^{\ddagger}{}_{R,X})_R = \tfrac{1}{2}d(\Delta E^{\ddagger}{}_{R,R})_R = \tfrac{1}{2}[d(E(R\text{--}H\text{--}R))_R - d(E(R))_R - d(E(R\text{–}H))_R]$$

Here, $d(E(R\text{--}H\text{--}R))_R$, $d(E(R))_R$, and $d(E(R\text{–}H))_R$ represent the energy variations of the TS, $R^{\bullet}$, and R–H with the change in R, respectively. Similarly, for the variation in $\Delta E_{R,X}$

$$d(\Delta E_{R,X})_R = d(E(R))_R - d(E(R\text{–}H))_R$$

Then $\alpha_I$ is given by

---

(29) Murdoch, J. R. *J. Phys. Chem.* **1983**, *87*, 1571.

(30) Murdoch, J. R.; Gryson, J. A.; McMiller, D. F. *J. Am. Chem. Soc.* **1982**, *104*, 600.

(31) Arnett, E. M.; Reich, R. *J. Am. Chem. Soc.* **1980**, *102*, 5892.

(32) Yamataka, H.; Nagase, S.; Ando, T.; Hanafusa, T. *J. Am. Chem. Soc.* **1986**, *108*, 601.

(33) (a) Bordwell, F. G.; Boyle, W. J., Jr.; Hautala, J. A.; Yee, K. C. *J. Am. Chem. Soc.* **1969**, *91*, 4002. (b) Bordwell, F. G.; Boyle, W. J. *J. Am. Chem. Soc.* **1972**, *94*, 3907.

$$\alpha_I = d(\Delta E_0{}^{\ddagger}{}_{R,X})_R/d(\Delta E_{R,X})_R = [d(E(R\text{--}H\text{--}R))_R - d(E(R))_R - d(E(R\text{–}H))_R]/(2[d(E(R))_R - d(E(R\text{–}H))_R]) = [d(E(R))_R - d(E(R\text{–}H))_R + d(E(R\text{--}H\text{--}R))_R - 2d(E(R))_R]/(2[d(E(R))_R - d(E(R\text{–}H))_R]) = \frac{1}{2}\left[1 - \frac{2d(E(R))_R - d(E(R\text{--}H\text{--}R))_R}{d(E(R))_R - d(E(R\text{–}H))_R}\right] \quad (13)$$

When $d(E(R\text{--}H\text{--}R))_R$ can be approximated by $2d(E(R))_R$, the numerator of the second term of eq 13 becomes zero, making $\alpha_I = 0.5$. When $d(E(R\text{--}H\text{--}R))_R$ can be approximated by $2d(E(R\text{–}H))_R$, $\alpha_I$ becomes −0.5; similarly when $d(E(R\text{--}H\text{--}R))_R$ is equal to $d(E(R))_R + d(E(R\text{–}H))_R$, $\alpha_I$ becomes zero. Thus, $\alpha_I$ is a function of the nature of the TS of the symmetry reaction in which perturbation is introduced. It may be regarded that $\alpha_I$ approaches 0.5 when the TS of the symmetry reaction becomes loose and that it approaches −0.5 when the TS becomes tight. In most examples illustrated in Figures 4–9 the size of $\alpha_I$ lies within this range.

The above discussion indicates that $\alpha_I$ can be taken as a measure of the tight–loose character of the TS of the symmetry reaction *provided that the arithmetic mean assumption is satisfied.* Note that the arithmetic mean assumption implies that there is no interaction between the two fragments in the TS (R and X in the reaction considered here) and that the R group at the TS has the same property both for the symmetry reaction and for the hypothetical thermoneutral reaction. This means that $\alpha_I$ may serve as an index of the nature of the TS of *the thermoneutral reaction* in the sense that it varies from −0.5 to 0.5, reflecting the resemblance of the TS to the product in terms of the response to energy perturbation on the R group.

In the reactions of R–H with H• (Figure 4a), the $\alpha_I$ value is 0.5, which indicates that the TS is very product-like in terms of the response to the energy perturbation. This can be rationalized by looking at the change of charge density on Me in going from the reactant to the TS or the product state for the parent reaction, Me–H + H• → Me• + $H_2$. Population analysis revealed that the charge density on the Me group is −0.20 e for Me–H while it is small both for the TS and Me• (−0.04 and 0.0 e, respectively).

**Anomaly in the Coefficient α.** Although in most cases the size of $\alpha_I$ lies between −0.5 and 0.5, it is large (0.8) in the reaction of R–H with Cl• (Figure 4b). An $\alpha_I$ value larger than 0.5 is an indication of the breakdown of the arithmetic mean assumption and suggests that the two fragments in the TS interact with each other. In the reaction shown in Figure 4b, it is conceivable that the TS, R--H--Cl, has considerable polar character because of the electronegativity difference between the R group and the Cl atom. The population analysis of the TS (R = Me) indeed showed that the Me group is positively charged by 0.10 e while the Cl atom is negatively charged by 0.21 e. The results can be compared with those of the two TSs, Me--H--H and Me--H--Me, as well as the complex, Me---HCl; in these cases the Me group is slightly negatively charged by about 0.04 e. Thus, the amount of charge on Me for the reaction with X = H is

| Me | ---- H ---- | Cl | Me | ---- H ---- | H | Me | ---- H ---- | Me |
|---|---|---|---|---|---|---|---|---|
| +0.10 | +0.11 | −0.21 | −0.04 | +0.04 | 0.00 | −0.05 | +0.10 | −0.05 |

| Me | --- H | -Cl |
|---|---|---|
| −0.03 | +0.24 | −0.21 |

essentially the same as that for the corresponding symmetry reaction, while that for the reaction with X = Cl is different. The interaction between Me and Cl is the origin of this charge separation, which is not present in either the initial or the final state, and the charge separation is responsible for the large α value for this reaction.

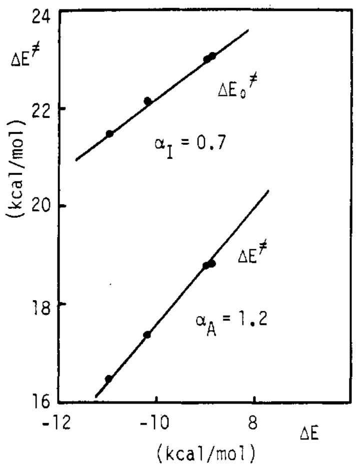

**Figure 10.** Plots of $\Delta E^{\ddagger}$ and $\Delta E_0{}^{\ddagger}$ vs $\Delta E$ for the reactions of $ArCH(CH_3)NO_2$ with $^-OH$ in water.[27,33b]

A similar apparent anomaly was experimentally observed in the deprotonation of arylnitroethane (eq 14).[33]

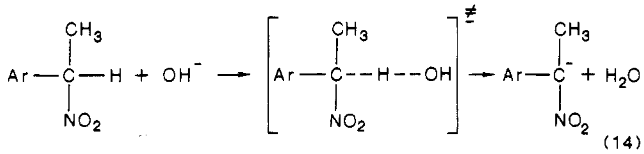

$$ArC(CH_3)(NO_2)\text{—}H + OH^- \rightarrow [ArC(CH_3)(NO_2)\text{--}H\text{--}OH]^{\neq} \rightarrow ArC^-(CH_3)(NO_2) + H_2O \quad (14)$$

As can be seen in Figure 10, $\alpha_A$ in this reaction is larger than unity due to large $\alpha_I$, and $\alpha_C$ is 0.5, a situation similar to the present reaction (X = Cl).

A series of reactions of 9-substituted fluorene with 9-alkylfluorenyl anion is another system that gives large $\alpha_A$ values (eq 15).[30] Here, R and R′ are H, Me, Et, *i*-Pr, or *t*-Bu.

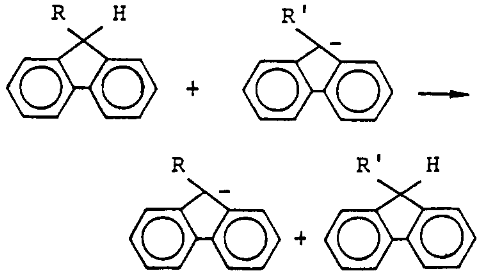

(15)

The $\alpha_A$ values based on the variation in R are 0.7, 0.8 1.3, 1.6, and 1.8 for R′ = H, Me, Et, *i*-Pr, and *t*-Bu, respectively. The $\alpha_I$ values are 0.2, 0.3, 0.8, 1.1, and 1.3, respectively, for the same series of reactions. The $\alpha_C$ values are again 0.5 in these cases. The magnitudes and the R′ dependence of $\alpha_I$ clearly indicate that there is new interaction between the two fluorenyl groups in the TS. Direct steric interaction or steric effect on solvation may account for this interaction.[30]

## Summary

The results of the present computational test and the analysis in terms of Marcus' theory can be summarized as follows. (1) A variation in the TS structure is not simply determined by variations in $\Delta E$, $\Delta E^{\ddagger}$, and $\Delta E_0{}^{\ddagger}$; the nature of the TS is an important factor in controlling the extent of the TS variation. A transition-state index such as Miller's $X^*$ is not always a reliable measure of the TS structure. (2) The apparent $\alpha_A$ value is an experimentally (or computationally) derived index of selectivity, i.e., reactant-like or product-like character in terms of the response to energy perturbation, but it is not necessarily a measure of the structure of the TS even though it shows a normal magnitude. Selectivity and the structure of the TS are different matters. (3) The intrinsic barrier is in most cases not constant for a series of reactions but varies linearly with the change in endothermicity. $\alpha_A$ is controlled in large part by the variation of $\alpha_I$ and can be a TS index in a conventional sense only when $\Delta E_0^{\ddagger}$ is constant for a series of reactions. The $\alpha_I$ value is a measure of the tight–loose character of the TS of the symmetry reaction, provided that the arithmetic mean assumption holds. (4) The $\alpha_A$ value can be outside the normal range when the arithmetic mean assumption breaks down, which may occur due to a new interaction between the two reacting fragments in the TS.

**Acknowledgment.** We thank Professor Y. Kondo of Osaka University for critical discussions. Numerical calculations were carried out at the Computer Center of the Institute for Molecular Science, using the GAUSSIAN 80[12] and GAUSSIAN 82[13] programs in the Computer Center library package.

**Registry No.** $HCH_3$, 74-82-8; $HCH_2CH_3$, 74-84-0; $HCH(CH_3)_2$, 74-98-6; $HC(CH_3)_3$, 75-28-5; H·, 12385-13-6; Cl·, 22537-15-1.

---

# Isoquinolinium Salt Syntheses from Cyclopalladated Benzaldimines and Alkynes

Guangzhong Wu, Steven J. Geib, Arnold L. Rheingold, and Richard F. Heck*

*Department of Chemistry and Biochemistry and the Center for Catalytic Science and Technology, University of Delaware, Newark, Delaware 19716*

*Received September 15, 1987*

Cyclopalladated, N-substituted benzaldimine tetrafluoroborates react with disubstituted alkynes in poor to good yields to form isoquinolinium tetrafluoroborates. The reaction is particularly useful for preparing N,3,4-trisubstituted products. Electron-donating substituents may be present at the 5, 6, 7, and 8 positions, as well. Methyl (*p*-benzoxyphenyl)propiolate adds to cyclopalladated *N*-methyl-3-benzoxy-4-methoxybenzaldimine tetrafluoroborate to form the 3-arylisoquinolinium salt. 3-Hexyne reacts with cyclopalladated *N*-phenylbenzaldimine chloro dimer at 150 °C to form the isoquinolinium chloride but at less than half (29%) the yield that is obtained from the corresponding tetrafluoroborate.

The presence of the isoquinoline ring system in many natural alkaloids has led to the development of a variety of methods for its synthesis. Of the many methods, however, only three are commonly employed: the Bischler–Napieralski, the Pictet–Pengler, and the Pomeranz–Fritsch reactions.[1] Both the Bischler–Napieralski and Pomeranz–Fritsch methods use strong acids in the ring closures limiting the procedures to acid-stable reactants. The Pictet–Spengler transformation often can be achieved under very mild conditions but a disadvantage of this method may be a tedious preparation of the starting material, an appropriately substituted phenylethylamine.

More recently a method based upon cyclopalladated *tert*-butylarylaldimines has been reported.[2] This synthesis, however, has as a final step a pyrolysis at 180–200 °C which also limits its utility. We have discovered a related, new synthesis of the isoquinoline ring system which occurs under mild, neutral conditions also starting with generally easily available aromatic imines. The method, which is modeled after our cinnolinium salt synthesis,[3,4] is very suitable for preparing polysubstituted and hindered derivatives.

## Results and Discussion

Cyclopalladated arylaldimine tetrafluoroborates react with various disubstituted alkynes to form 3-, 4-, and N-substituted isoquinolinium tetrafluoroborates in low to good yields. Additional substituents may be present in

**Table I. Isoquinolinium Salt Preparations**

| complex 1,[a] $R^1$ = | alkyne 2, $R^2$ = | temp (°C) and time of alkyne addition (h) | product 3, % yield |
|---|---|---|---|
| $C_6H_5$ | $C_2H_5$ | 100, 2 | 80 |
| $C_6H_5$ | $CH_3O_2C$ | 100, 5 | 25 |
| $C_6H_5$ | $(C_2H_5O)_2CH$ | 100, 4 | 12 |
| $o$-$CH_3C_6H_4$ | $C_2H_5$ | 100, 2 | 60 |
| $o$-$CH_3C_6H_4$ | $C_2H_5$ | 25,[b] | 5 |
| $C_6H_5CH_2$ | $C_2H_5$ | 100, 1 | 42 |
| $C_6H_5CH_2$ | $C_2H_5$ | 25,[b] | trace |
| $C_6H_5CH_2$ | $C_2H_5$ | 100, 3 | 64 |
| $C_6H_5CH_2$ | $C_6H_5$ | 100, 1 | 34 |
| $CH_3$ | $C_6H_5$ | 100, 1 | 17[c] |
| $CH_3$ | $C_2H_5$ | 100,[b] | ~0 |
| $t$-$C_4H_9$ | $C_6H_5$ | 100, 2 | 27 |
| $CH_3$[d] | $C_6H_5$ | 100, 1 | 48[e] |
| $CH_3$[d] | $C_6H_5$ | 70, 1 | 66[e] |
| $CH_3$[f] | $C_2H_5$ | 100, 1 | 45[g] |
| $CH_3$[f] | 4-$PhCH_2OC_6H_4$ and $CO_2CH_3$ | 100, 1 | 54[g] |
| $CH_3$[f] | 4-$PhCH_2OC_6H_4$ and $CO_2CH_3$ | 100, 4 | 53[g] |
| $p$-$CH_3C_6H_4$[i] | $C_2H_5$ | 100, 1 | 80[j,k] |
| $p$-$CH_3C_6H_4$[i] | $C_6H_5$ | 100, 2 | 75[k] |

[a] All prepared in nitromethane solution from the dimeric chloro complexes and silver tetrafluoroborate and used without isolation. [b] Alkyne all present initially in methylene chloride solution. [c] Complex was unstable at 100 °C (see text). [d] Complex is the 3,6-dimethoxy derivative. [e] Product is the 5,8-dimethoxy derivative. [f] Complex is the 4-methoxy-5-benzoxy derivative. [g] Product is the 6-methoxy-7-benzoxy derivative. [h] Product is the 2-methyl-3-(*p*-benzoxyphenyl)-4-(methoxycarbonyl)-6-methoxy-7-benzoxyisoquinolinium tetrafluoroborate. [i] Complex is the 4-nitro derivative. [j] 60% of the complex was recovered. [k] Product is totally oligomers.

---

[1] *Organic Reactions* John Wiley Sons: London, Sydney, 1951; Vol. VI, Chapters 2, 3 and 4.

[2] Girling, I. R.; Widdowson, D. A. *Tetrahedron Lett.* **1982**, *23*, 4281.

[3] Wu, G.; Rheingold, A. L.; Heck, R. F. *Organometallics* **1986**, *5*, 1922.

[4] Wu, G.; Rheingold, A. L.; Heck, R. F. *Organometallics* **1987**, *6*, 1941.

0022-3263/88/1953-3238$01.50/0 © 1988 American Chemical Society